Improved Muscle Wrapping Algorithms Using Explicit Path-Error Jacobians

Andreas Scholz, Ian Stavness, Michael Sherman, Scott Delp, and Andrés Kecskeméthy

Abstract Muscle wrapping computations are an important feature in musculoskeletal simulations. In this paper we present a novel Jacobian-based method for line-based muscle-path computations over multiple general smooth surfaces allowing for second-order Newton-Raphson iterations. The method is based on the analytical determination of infinitesimal displacements along geodesics using Jacobi fields. It does not share the disadvantages of discretized methods in terms of non-smoothness when using surface discretizations, and high computational costs when using discretized spring-mass approaches. The paper focusses on the technical details of the proposed method, while specific biomechanical applications are left for future contributions. An example with three surfaces involving a surface with a general distribution of curvature shows the general applicability of the method.

Key words: Muscle wrapping, Jacobi fields, geodesics.

1 Introduction

A key task of musculoskeletal simulations is the computation of the transmission of tensional muscle force to joint moments and/or reaction forces. Muscles are commonly modeled as thin strings which take the locally shortest path between their origin and insertion points while wrapping frictionlessly around multiple wrapping surfaces that represent neighboring bones, tissue,

Andreas Scholz, Andrés Kecskeméthy
University of Duisburg-Essen e-mail: {scholz.andreas, andres.kecskemethy}@uni-due.de
Ian Stavness
University of Saskatchewan e-mail: stavness@gmail.com
Michael Sherman, Scott Delp
Stanford University e-mail: {msherman, delp}@stanford.edu

and the neglected dimensions of the muscle. State-of-the-art approaches to line-based muscle wrapping can be divided into two main groups: (1) approaches using surface or path discretizations and (2) approaches using explicit smooth surfaces. Discretizing approaches such as [1, 2] yield fast approximate solutions and allow for using realistic bone geometry obtained from MRI or CT. However, they cause nonsmooth path motion at surface edges and hence only C^1 continuous behavior of the path length, which slows down variable-step-size integrators in dynamic simulations driven by muscle forces. Explicit smooth wrapping-surface approaches such as [3, 4, 5] provide continuous wrapping, but are limited to simple objects such as single spheres, single cylinders, or a compound of both, which are not always sufficient to represent general bone and surrounding soft tissue surfaces. Elastic approaches such as [4] circumvent this problem, but introduce new difficulties such as an oscillatory behavior of the muscle path. Recently, Stavness et al. 2012 [6] proposed a root-finding approach in which the total path is regarded as a concatenation of straight-line segments between geodesics on the surfaces, allowing to tackle general smooth surfaces while avoiding oscillatory behavior. The path is computed by iterating the positions of the boundary points of the geodesics until all transitions between adjacent segments are collinear. To this end, the Jacobian mapping variations of geodesic boundary points to variations of the path error is required. While this Jacobian can be determined by finite differences, such discretizations are expensive and also do not render smooth transitions between time steps. In this paper, we derive, based on the formulation [6], explicit formulas for the path-error Jacobian using differential-geometric properties of infinitesimal displacements along geodesics based on Jacobi fields. The approach is easy to implement, yields fast convergence and is thus well-suited for muscle wrapping applications.

2 Conditions for a geodesic over several surfaces

We regard a string that is spanned between an origin point O and an insertion point I. The string wraps frictionlessly across a set of n wrapping surfaces $\mathcal{S}^i$ $(i = 1, \dots, n)$ and minimizes the length with respect to all other neighboring trajectories connecting O and I. The total muscle path results as a concatenation of $n-1$ straight-line segments between the surfaces, two straight lines to points O and I, and n geodesics on the surfaces. Each geodesic γ^i is uniquely defined by its start point P^i and end point Q^i, and each straight-line segment is defined by the unit direction vector $\underline{e}^i$ and its respective boundary points Q^{i-1} and P^i for $1 < i < n+1$, O and P^1 for $i = 1$ and Q^n and I for $i = n+1$.

Assume that the section of interest of surface $S^i \in \mathbb{R}^3$ can be parameterized by a nonsingular differentiable function $\underline{x}^i(u^i, v^i) : \mathbb{R}^2 \mapsto \mathbb{R}^3$ with respect to a surface base frame $\mathcal{K}^i_{\mathcal{S}}$ in terms of two surface coordinates $(u^i, v^i) \in \mathbb{R}^2$ such that for the outwards normal it holds (Fig. 1)

$$\underline{N}^i := \frac{\underline{x}_u^i \times \underline{x}_v^i}{\| \underline{x}_u^i \times \underline{x}_v^i \|}, \quad \underline{x}_{(.)} := \frac{\partial \underline{x}}{\partial (.)}. \tag{1}$$

Moreover, let $\underline{t}^i$ be the geodesic's tangent and let $\underline{B}^i = \underline{t}^i \times \underline{N}^i$ be its binormal.

At the solution configuration, all transitions between adjacent segments are collinear (see Fig. 1). If they are not, for each geodesic γ^i, four possible local path errors arise from the orthogonality conditions

$$\underline{\varepsilon}^i(\underline{q}^i, \mathcal{K}_\mathcal{S}^i) := \begin{bmatrix} \underline{e}^i \cdot \underline{N}_P^i \\ \underline{e}^i \cdot \underline{B}_P^i \\ \underline{e}^{i+1} \cdot \underline{N}_Q^i \\ \underline{e}^{i+1} \cdot \underline{B}_Q^i \end{bmatrix}, \quad \underline{q}^i = \begin{bmatrix} u_P^i \\ v_P^i \\ u_Q^i \\ v_Q^i \end{bmatrix}. \tag{2}$$

The local path errors can be assembled into the global path-error vector

$$\underline{\varepsilon}(\underline{q}, \mathcal{K}) = \begin{bmatrix} \underline{\varepsilon}^1 \\ \underline{\varepsilon}^2 \\ \vdots \\ \underline{\varepsilon}^n \end{bmatrix} \in \mathbb{R}^{4n \times 1}, \quad \underline{q} = \begin{bmatrix} \underline{q}^1 \\ \underline{q}^2 \\ \vdots \\ \underline{q}^n \end{bmatrix} \in \mathbb{R}^{4n \times 1}, \quad \mathcal{K} = \begin{bmatrix} \mathcal{K}_\mathcal{S}^1 \\ \mathcal{K}_\mathcal{S}^2 \\ \vdots \\ \mathcal{K}_\mathcal{S}^n \end{bmatrix}. \tag{3}$$

yielding the nonlinear root condition for the muscle path

$$\underline{\varepsilon}(\underline{q}, \mathcal{K}) = \underline{0}. \tag{4}$$

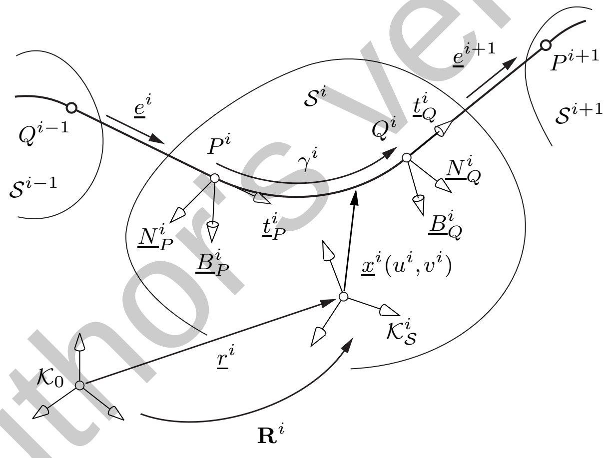

Fig. 1 Global path error components

For each time step, the set of reference frames contained in $\mathcal{K}$ is fixed, and Eqn. (4) can be solved for the unknown geodesic boundary-point coordinates $\underline{q}$ using a Newton-Raphson method. This requires knowledge of the Jacobian $\mathbf{J}_q := \partial \underline{\varepsilon} / \partial \underline{q} \in \mathbb{R}^{4n \times 4n}$ containing the partial derivatives

$$
\mathbf{J}_q = \begin{bmatrix}
\frac{\partial \underline{\varepsilon}^1}{\partial \underline{q}_P^1} & \frac{\partial \underline{\varepsilon}^1}{\partial \underline{q}_Q^1} & \frac{\partial \underline{\varepsilon}^1}{\partial \underline{q}_P^2} & & & & & & & & \\
& \frac{\partial \underline{\varepsilon}^2}{\partial \underline{q}_Q^1} & \frac{\partial \underline{\varepsilon}^2}{\partial \underline{q}_P^2} & \frac{\partial \underline{\varepsilon}^2}{\partial \underline{q}_Q^2} & \frac{\partial \underline{\varepsilon}^2}{\partial \underline{q}_P^3} & & & & & & \\
& & \ddots & \ddots & \ddots & \ddots & & & & & \\
& & & \frac{\partial \underline{\varepsilon}^i}{\partial \underline{q}_Q^{i-1}} & \frac{\partial \underline{\varepsilon}^i}{\partial \underline{q}_P^i} & \frac{\partial \underline{\varepsilon}^i}{\partial \underline{q}_Q^i} & \frac{\partial \underline{\varepsilon}^i}{\partial \underline{q}_P^{i+1}} & & & & \\
& & & & \ddots & \ddots & \ddots & \ddots & & & \\
& & & & & \frac{\partial \underline{\varepsilon}^{n-1}}{\partial \underline{q}_Q^{n-2}} & \frac{\partial \underline{\varepsilon}^{n-1}}{\partial \underline{q}_P^{n-1}} & \frac{\partial \underline{\varepsilon}^{n-1}}{\partial \underline{q}_Q^{n-1}} & \frac{\partial \underline{\varepsilon}^{n-1}}{\partial \underline{q}_P^{n}} & \\
& & & & & & & \frac{\partial \underline{\varepsilon}^n}{\partial \underline{q}_Q^{n-1}} & \frac{\partial \underline{\varepsilon}^n}{\partial \underline{q}_P^n} & \frac{\partial \underline{\varepsilon}^n}{\partial \underline{q}_Q^n}
\end{bmatrix} \tag{5}
$$

A general block-row $\mathbf{J}_q\,(i,:)$ in Eqn. (5) comprises four submatrices

$$
\mathbf{J}_q\,(i,:) = \begin{bmatrix} \frac{\partial \underline{\varepsilon}^i}{\partial \underline{q}_Q^{i-1}} & \frac{\partial \underline{\varepsilon}^i}{\partial \underline{q}_P^i} & \frac{\partial \underline{\varepsilon}^i}{\partial \underline{q}_Q^i} & \frac{\partial \underline{\varepsilon}^i}{\partial \underline{q}_P^{i+1}} \end{bmatrix} \tag{6}
$$

which represent two coupling terms $\partial \underline{\varepsilon}^i / \partial \underline{q}_Q^{i-1}$ if $i > 1$, and $\partial \underline{\varepsilon}^i / \partial \underline{q}_P^{i+1}$ if $i < n$, as well as the local path-error Jacobians $\mathbf{J}_q^i := \partial \underline{\varepsilon}^i / \partial \underline{q}^i$

$$
\mathbf{J}_q^i = \begin{bmatrix}
\frac{\partial}{\partial u_P^i}\left(\underline{e}^i \cdot \underline{N}_P^i\right) & \frac{\partial}{\partial v_P^i}\left(\underline{e}^i \cdot \underline{N}_P^i\right) & \frac{\partial}{\partial u_Q^i}\left(\underline{e}^i \cdot \underline{N}_P^i\right) & \frac{\partial}{\partial v_Q^i}\left(\underline{e}^i \cdot \underline{N}_P^i\right) \\
\frac{\partial}{\partial u_P^i}\left(\underline{e}^i \cdot \underline{B}_P^i\right) & \frac{\partial}{\partial v_P^i}\left(\underline{e}^i \cdot \underline{B}_P^i\right) & \frac{\partial}{\partial u_Q^i}\left(\underline{e}^i \cdot \underline{B}_P^i\right) & \frac{\partial}{\partial v_Q^i}\left(\underline{e}^i \cdot \underline{B}_P^i\right) \\
\frac{\partial}{\partial u_P^i}\left(\underline{e}^{i+1} \cdot \underline{N}_Q^i\right) & \frac{\partial}{\partial v_P^i}\left(\underline{e}^{i+1} \cdot \underline{N}_Q^i\right) & \frac{\partial}{\partial u_Q^i}\left(\underline{e}^{i+1} \cdot \underline{N}_Q^i\right) & \frac{\partial}{\partial v_Q^i}\left(\underline{e}^{i+1} \cdot \underline{N}_Q^i\right) \\
\frac{\partial}{\partial u_P^i}\left(\underline{e}^{i+1} \cdot \underline{B}_Q^i\right) & \frac{\partial}{\partial v_P^i}\left(\underline{e}^{i+1} \cdot \underline{B}_Q^i\right) & \frac{\partial}{\partial u_Q^i}\left(\underline{e}^{i+1} \cdot \underline{B}_Q^i\right) & \frac{\partial}{\partial v_Q^i}\left(\underline{e}^{i+1} \cdot \underline{B}_Q^i\right)
\end{bmatrix} \tag{7}
$$

In this Jacobian, the derivatives of the normal vectors $\underline{N}_P^i, \underline{N}_Q^i$ as well as of the unit vectors $\underline{e}^i, \underline{e}^{i+1}$ with respect to the coordinates u_P^i, v_P^i and u_Q^i, v_Q^i can be determined directly from local surface geometry. These derivations are left out here due to lack of space. On the other hand, the partial derivatives of the geodesic's binormals $\underline{B}_P^i$ and $\underline{B}_Q^i$ require through their definition $\underline{B}^i = \underline{t}^i \times \underline{N}^i$ the partial derivatives of the tangent vectors $\underline{t}_P^i$ and $\underline{t}_Q^i$ with respect to the coordinates of both geodesic boundary points. These derivatives involve cross-over differential mappings over geodesics which can be computed using Jacobi fields, as discussed next.

3 Coupled End-Point Derivatives Across Geodesics

In this section, we review some fundamental concepts of differential geometry (see [7, 8]) and apply them to the given problem. Let the geodesic γ be given in polar form, i.e. assume that the start point P is fixed. Let s be the arc length of γ and let θ be an angular coordinate defining the initial direction of γ (Fig. 2). By the Lemma of Gauss it holds $\mathrm{F}_{\mathrm{polar}} = \underline{x}_\theta \cdot \underline{x}_s = 0 \;\forall\; s \neq 0$.

When the angle θ is varied, a point Q at some constant distance from the pole P will travel an arc length β_Q along a geodesic circle. We define the positive arc direction of such a circle to be oriented along the binormal vector $\underline{B}_Q$ at Q. The partial derivative $a = \partial\beta/\partial\theta$ of the arc length β at any point of the geodesic fulfills the scalar Jacobi equation (see [7, 9])

$$a'' + K\,a = 0\,, \quad a(s=0) = 0\,, \quad a'(s=0) = 1\,, \quad (.)' := \partial(.)/\partial s\,, \qquad (8)$$

where K is the Gaussian curvature. The scalar Jacobi Eqn. (8) can be integrated together with the differential equations of the geodesic.

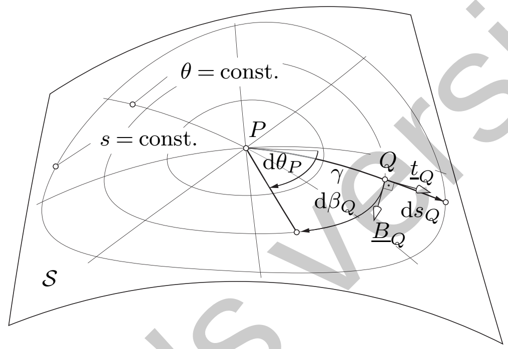

Fig. 2 Geodesic polar coordinates (θ, s) for a fixed pole P

For the computation of the partial derivatives of the tangent vectors with respect to the boundary-point coordinates, a local coordinate-transformation is carried out first. Let $\mathrm{d}s_Q$ and $\mathrm{d}\beta_Q$ be infinitesimal increments along the geodesic γ and the geodesic circle at point Q for the fixed pole P (Fig. 2). Likewise, let $\mathrm{d}s_P$ and $\mathrm{d}\beta_P$ be the infinitesimal increments along the geodesic and the geodesic circle at point P when Q is taken as the fixed pole. Here, $\mathrm{d}s_P$ is oriented along $\underline{t}_P$, i.e. in direction of length shortening, while $\mathrm{d}\beta_P$ is oriented along $\underline{B}_P$. Locally, the transformation of the differentials of β, s and u, v is given by

$$\frac{\partial s}{\partial u} = \underline{x}_u \cdot \underline{t}\,, \quad \frac{\partial s}{\partial v} = \underline{x}_v \cdot \underline{t}\,, \quad \frac{\partial \beta}{\partial u} = \underline{x}_u \cdot \underline{B}\,, \quad \frac{\partial \beta}{\partial v} = \underline{x}_v \cdot \underline{B}\,. \qquad (9)$$

The derivatives of $\underline{t}_P$ and $\underline{t}_Q$ with respect to s_P and s_Q can be obtained from the Frenet-Serret formulas (see, e.g. [8])

$$\frac{\partial \underline{t}_P}{\partial s_P} = \kappa_P \, \underline{n}_P \,, \quad \frac{\partial \underline{t}_P}{\partial s_Q} = \underline{0}, \quad \frac{\partial \underline{t}_Q}{\partial s_P} = \underline{0}, \quad \frac{\partial \underline{t}_Q}{\partial s_Q} = \kappa_Q \, \underline{n}_Q \,, \tag{10}$$

where $\underline{n}_P := \underline{x}''_P/\kappa_P$ and $\underline{n}_Q := \underline{x}''_Q/\kappa_Q$ are the unit normals of the geodesic and κ_P and κ_Q are the curvatures of the geodesic at P and Q.

The concept of the Jacobi field along the geodesic γ allows for the computation of the derivatives of $\underline{t}_P$ and $\underline{t}_Q$ with respect to β_P and β_Q. For an infinitesimal motion $\mathrm{d}\beta_Q$ of the geodesic's end point Q, the tangent vector $\underline{t}_P$ at the start point P rotates about the surface normal $\underline{N}_P$ with an angle $\mathrm{d}\theta_P$. This relation is given by the scalar Jacobi field at Q, yielding

$$\frac{\partial \underline{t}_P}{\partial \beta_Q} = \frac{\partial \underline{t}_P}{\partial \theta_P}\frac{\partial \theta_P}{\partial \beta_Q} = \underline{B}_P \, a_Q^{-1} \,. \tag{11}$$

Here $\partial \underline{t}_P/\partial \theta_P$ is a local derivative, while $\partial \theta_P/\partial \beta_Q$ depends on the geodesic. Note that the latter term becomes singular at conjugate points of P, which are defined by a vanishing Jacobi field $a = 0$. Analogously, symmetry yields

$$\frac{\partial \underline{t}_Q}{\partial \beta_P} = \frac{\partial \underline{t}_Q}{\partial \theta_Q}\frac{\partial \theta_Q}{\partial \beta_P} = -\underline{B}_Q \, \hat{a}_P^{-1} \,, \tag{12}$$

where $\hat{a}$ denotes the "backwards" Jacobi field obtained by integrating Eqn. (8) from Q to P.

The other derivatives are obtained similarly using the definition $\underline{t} = \partial \underline{x}/\partial s$

$$\frac{\partial \underline{t}_P}{\partial \beta_P} = \frac{\partial \underline{t}_P}{\partial \theta_Q}\frac{\partial \theta_Q}{\partial \beta_P} = \frac{\partial}{\partial \theta_Q}\left(\frac{\partial \underline{x}_P}{\partial s_P}\right)\hat{a}_P^{-1} \tag{13}$$

and the theorem of Schwarz, yielding

$$\frac{\partial \underline{t}_P}{\partial \beta_P} = \frac{\partial}{\partial s_P}\left(\frac{\partial \underline{x}_P}{\partial \theta_Q}\right)\hat{a}_P^{-1} = \frac{\partial}{\partial s_P}\left(\underline{B}_P \, \hat{a}_P\right)\hat{a}_P^{-1} = -\tau_P \, \underline{N}_P - \underline{B}_P \, \hat{a}'_P \, \hat{a}_P^{-1} \,, \tag{14}$$

where τ is the geodesic's torsion. Likewise, it holds by symmetry

$$\frac{\partial \underline{t}_Q}{\partial \beta_Q} = -\tau_Q \, \underline{N}_Q + \underline{B}_Q \, a'_Q \, a_Q^{-1} \,. \tag{15}$$

4 Results

The formulas described above can be assembled into a modular program for muscle-path computations. Here we show the results of our implementation in

Matlab. In this implementation, the muscle path can be spanned over several general surfaces (Fig. 3a), and both the end points as well as all surfaces can perform arbitrary spatial motions. Each time frame comprises two types of iterations: an inner loop and an outer loop. The inner loop carries out geodesic shooting from point P such that point Q is reached. Each iteration step consists of numerically integrating the geodesic equations and Eqn. (8) with given initial direction θ. Corrections of the geodesic length and the initial direction are obtained by projecting the difference $\Delta\underline{x}_E = \underline{x}_Q - \underline{x}_E$ from the current trial end point E to the target point Q onto the two polar directions at E

$$\Delta s_E = \Delta\underline{x}_E \cdot \underline{t}_E \tag{16}$$
$$\Delta\theta_P = \Delta\underline{x}_E \cdot \underline{B}_E\, a_E^{-1}\,. \tag{17}$$

The outer loop carries out the Newton-Raphson iteration for path error $\underline{\varepsilon}^{(k)}$

$$\underline{q}^{(k+1)} = \underline{q}^{(k)} - \left[\mathbf{J}_q^{(k)}\right]^{-1} \underline{\varepsilon}^{(k)}\,. \tag{18}$$

Figure 3a shows a sample motion with three surfaces, where S^3 represents the case of a general distribution of curvature and where the nonsymmetric ellipsoid S^2 is rotating about a skew axis. Due to the closedness of subsequent time frames, both loops converge in 2-3 iterations per frame. Figure 3b shows one inner loop for $\mathcal{S}^2$. Figure 3c contains the time histories of total muscle length and its rate of length change, showing that both curves are smooth.

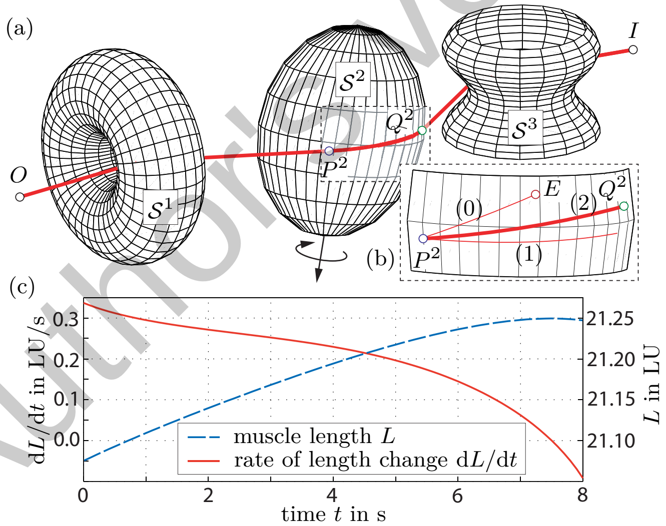

Fig. 3 (a) Sample application; (b) Inner-loop iterations using Eqns. (16, 17); (c) Smooth muscle length and rate of length change

5 Conclusions

The presented approach is suitable for efficient smooth muscle-wrapping based on second-order Newton iterations. The path-error Jacobian can be determined explicitly by solving the Jacobi field Eqn. (8). Second-order convergence can be achieved for inner loop geodesic shooting iterations using geodesic polar coordinates. The algorithms are operational for an arbitrary number of surfaces which can be parameterized explicitly. Future publications will provide a comparison to existing approaches and the application to specific biomechanics examples, and may involve the generalization of the formulation to multiple-patch as well as to implicit surface parametrizations.

Acknowledgements

Adrian Butscher, Leonidas Guibas, Justin Solomon, and Matthew Millard. This work was supported by the German National Academic Foundation, the Natural Sciences and Engineering Research Council of Canada, and NIH grants U54 GM072970 (Simbios) and R24 HD065690 (NCSRR).

References

1. E. Desailly, P. Sardain, N. Khouri, D. Yepremian, and P. Lacouture. The convex wrapping algorithm: A method for identifying muscle paths using the underlying bone mesh. *Journal of Biomechanics*, 43:2601–2607.
2. F. Gao, M. Damsgaard, J. Rasmussen, and S. T. Christensen. Computational method for muscle-path representation in musculoskeletal models. *Biological Cybernetics*, 87:199–210, 2002.
3. I. W. Charlton and G. R. Johnson. Application of spherical and cylindrical wrapping algorithms in a musculoskeletal model of the upper limb. *Journal of Biomechanics*, 34:1209–1216, 2001.
4. S. P. Marsden, D. C. Swailes, and G. R. Johnson. Algorithms for exact multi-object muscle wrapping and application to the deltoid muscle wrapping around the humerus. *Proceedings of the Institution of Mechanical Engineers. Part H, Journal of Engineering in Medicine*, 222(7):1081–1095, 2008.
5. B. A. Garner and M. G. Pandy. The obstacle-set method for representing muscle paths in musculoskeletal simulations. *Computer Methods in Biomechanics and Biomedical Engineering*, 3:1–30, 1998.
6. I. Stavness, M. Sherman, and S. L. Delp. A general approach to muscle wrapping over multiple surfaces. *Proceedings of the American Society of Biomechanics*, 2012.
7. M. P. Do Carmo. *Differential Geometry of Curves and Surfaces.* Prentice Hall, first edition, February 1976.
8. D. J. Struik. *Lectures on Classical Differential Geometry.* Dover Publications, Second edition, April 1988.
9. H. Thielhelm, A. Vais, D. Brandes, and F.-E. Wolter. Connecting geodesics on smooth surfaces. *The Visual Computer*, 28:529–539, 2012.